Relaxation dynamics of perturbed regular hyperbranched fractals

2010 J. Phys. A: Math. Theor. 43 105205

(http://iopscience.iop.org/1751-8121/43/10/105205)

J. Phys. A: Math. Theor. **43** (2010) 105205 (12pp) doi:10.1088/1751-8113/43/10/105205

Relaxation dynamics of perturbed regular hyperbranched fractals

Antonio Volta[1,2], **Mircea Galiceanu**[3] **and Aurel Jurjiu**[4]

[1] Theoretische Polymerphysik, Universität Freiburg, Hermann-Herder Straße 3, D-79104 Freiburg, Germany
[2] Dipartimento di Colture Arboree, University of Bologna, viale Fanin 46, I-40127 Bologna, Italy
[3] Departamento de Física, Universidade Federal do Paraná, 81531-990, Curitiba, PR, Brazil
[4] Universitatea Babes-Bolyai, Theoretical and Computational Physics, Simulation laboratory of nanostructured systems, Str. Mihail Kogalniceanu, nr. 1, 400084, Cluj-Napoca, Romania

E-mail: antonio.volta@unibo.it

Received 23 October 2009, in final form 28 January 2010
Published 22 February 2010
Online at stacks.iop.org/JPhysA/43/105205

Abstract
We focus on perturbed regular hyperbranched fractals (pRHF), which are RHF whose f coordinated centers (fCC) are traps. We compute the mechanical properties (storage and loss modulus) and the average displacement in the framework of generalized Gaussian structures, by making use of the eigenvalue spectrum of the connectivity matrix. We generalize the analysis to the case of a connectivity matrix perturbed by a diagonal and pure imaginary operator. Although the above-cited observables in this new situation lose their original meaning, they still give important information about the underlying structures and they could help to analyze other phenomena where complex operators are involved. We obtain analytically the eigenvalue spectrum for pRHF. A drastic change was observed in the behavior of the studied quantities even for a very small perturbation strength. However, it is still possible to depict the scaling of the fractals in the intermediate time (frequency) domains.

PACS numbers: 05.60.Gg, 05.40.−a, 66.20.Cy

(Some figures in this article are in colour only in the electronic version)

1. Introduction

One of the fundamental problems in polymer physics is to understand how the geometry of the macromolecules affects their dynamical behavior. This quest started with the fundamental works on dilute solutions for linear chains, pioneered by Rouse [1] and Zimm [2]. The results were extended to more and more complex architectures, i.e. star polymers [3, 4], dendrimers

[5–8], hyperbranched polymers [9–12] or small-world networks [13], by making use of the generalized Gaussian structures [14]. In this framework the structures consist of N beads, connected to each other by elastic springs with the elasticity constant K. The geometry is taken into account by connecting each bead to its nearest neighbors. For simplicity, all the beads will experience the same friction constant ζ with respect to the surrounding viscous medium (the solvent). Another assumption of the model is that the connecting springs behave harmonically, and thus the whole structure obeys Gaussian statistics. Many dynamical properties depend on the eigenvalue spectrum of their connectivity matrix $\mathbf{A}$ [14–16]. This is a real symmetric $N \times N$ matrix: the non-diagonal elements A_{nm} equal -1 if the the nth and mth beads are directly connected and 0 otherwise, while the diagonal elements A_{mm} equal the number of bonds emanating from the mth bead. The connectivity matrix was recently used to solve quantum mechanical problems by means of continuous time quantum walks (CTQWs) [17–19]. In quantum mechanics, the trapping problem was studied via a perturbative approach [20–22], i.e. in mathematical terms the transfer operator $\mathbf{T}$, normally assumed equal to the connectivity matrix, was slightly modified by adding to $\mathbf{A}$ a pure imaginary operator $\mathbf{\Gamma}$ acting as a dissipator; therefore, $\mathbf{T} = \mathbf{A_p} = \mathbf{A} + \mathbf{\Gamma}$. In this paper, we focus on regular hyperbranched fractals (RHFs) [11, 12] perturbed through $\mathbf{\Gamma}$, a normal regular hyperbranched fractal whose fCC are traps. In this case $\mathbf{\Gamma}$ is such that the off-diagonal elements Γ_{jk} fulfill $\Gamma_{jk} = 0$ and $\Gamma_{jj} = \mathrm{i}\gamma$ if j is a fCC and 0 otherwise. The operator $\mathbf{A_p}$ belongs to the class of complex symmetric operators that in the past few years acquired importance, since besides CTQWs, they found applications for studying some chemical problems such as the complex rotation method and the optical potential method, in which a scattering problem is reduced to a bound state problem in a non-Hermitian domain, see [27] and references therein. We perform a semi-analytical method able to obtain the full eigenvalue spectrum. We will focus on the relationship between the trap strength γ and the dynamical quantities, storage and loss modulus and the average displacement, in order to investigate the influence of the topology of the structures under study.

The paper is structured as follows: in section 2 we give a short description of the RHFs and then, in section 3, we study the spectrum of the fractals without or with traps for arbitrary functionality f and generation g. In section 4 we will derive new equations for the storage and the loss modulus (the real and the imaginary part of the complex shear modulus) and for the average displacement. Then, we will test these equations for perturbed RHFs. We noted that even a very small trap's strength will have a big influence on the final results. This paper will close with conclusions.

2. The structure

Figure 1 displays a RHF of functionality $f = 3$ and generations $g = 1, 2$ and 3. To build this structure one takes the object of generation $g = 1$, i.e. a star structure with the core connected by three branches to the external nodes. The next generation $g = 2$ is obtained by binding to the external nodes f identical copies of itself through f bonds; we obtain a new star-wise pattern of $(f + 1)^2$ nodes. By following this iteration procedure, a RHF of generation g will have $(f + 1)^g$ sites. The fractal dimension depends on the functionality f as follows:

$$\bar{d}_r = \frac{\ln(f + 1)}{\ln 3} \tag{1}$$

since increasing from the center the distance by a factor of 3 increases the number of sites inside it by $f + 1$. In figure 1 we highlight the position of the traps by open circles.

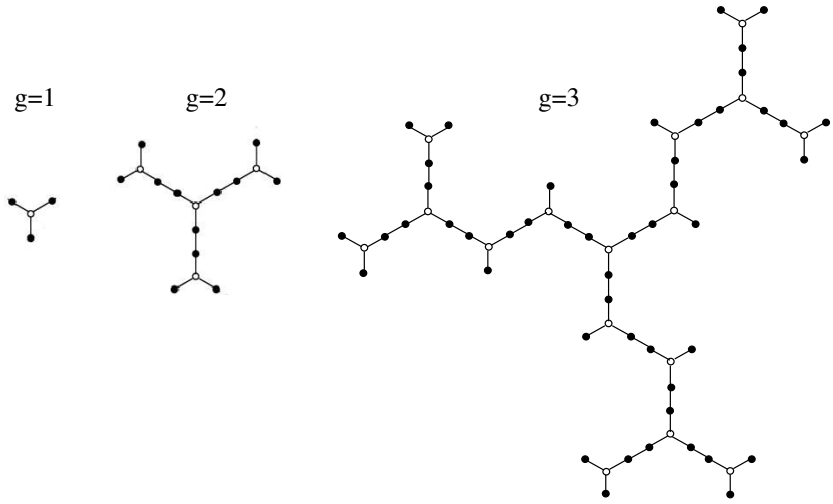

Figure 1. Regular hyperbranched fractal of functionality $f = 3$ and generations $g = 1, 2$ and 3. The traps are displayed by open circles.

3. Evaluation of the eigenvalues

3.1. Spectrum of RHF

For the unperturbed RHF, when there is no trap in the structure we found the eigenvalue spectrum of the connectivity matrix **A** by following an algebraic iterative procedure [11, 12]. The eigenvalue problem is reduced to the solution of cubic equations, due to the fact that the RHFs rescale under a real-space renormalization transformation [12, 25]. Knowing the eigenvalues of the RHFs of generation g, one obtains the eigenvalues of RHFs of generation $g + 1$ by

$$P\left(\lambda_i^{(g+1)}\right) = \lambda_i^{(g)}, \tag{2}$$

where $P(\lambda)$ is the polynomial:

$$P(\lambda) = \lambda(\lambda - 3)(\lambda - f - 1). \tag{3}$$

We set $P(\lambda) = a$ and equation (3) is recombined:

$$\lambda^3 - (f + 4)\lambda^2 + 3(f + 1)\lambda - a = 0. \tag{4}$$

Equation (4) can be solved analytically by introducing

$$p = \tfrac{1}{3}[f(f - 1) + 7] \tag{5}$$

$$q = \tfrac{1}{27}(5 - f)(f + 4)(2f - 1) \tag{6}$$

and

$$\rho = |p/3|^{3/2}. \tag{7}$$

The roots of equation (4) are then given by the Cardano solutions [28]:

$$\lambda_\nu = \frac{f + 4}{3} + 2\rho^{1/3} \cos\left[\frac{\mu + 2\pi\nu}{3}\right], \qquad \text{with} \quad \nu \in 1, 2, 3, \tag{8}$$

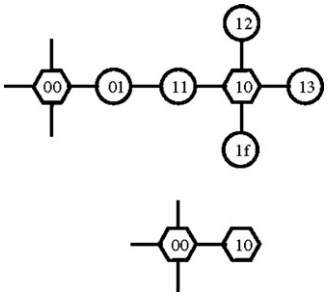

Figure 2. Decimation step for singly coordinated centers, following figure 14 of [12].

where

$$\mu = \arccos\left(\frac{a-q}{2\rho}\right). \tag{9}$$

In equation (4) we identify the constant a with λ_i^g, and by using equation (8), each non-zero eigenvalue of generation g will give rise to three new eigenvalues λ_i^{g+1}.

The non-degenerate eigenvalues include $\lambda = 0, \lambda = (f+1)$, and other eigenvalues generated by the 'seed' $\lambda = (f+1)$. For example, at the second generation of RHF we have five non-degenerate eigenvalues, i.e. $\lambda = 0$ and $\lambda = (f+1)$ and three eigenvalues obtained by substituting $a = (f+1)$ into equation (4). The degeneracy of the degenerate eigenvalues depends on the generation where they appeared for the first time. Thus, $\lambda = 1$, which is present due to $g = 1$, is the most degenerate eigenvalue with degeneracy given by

$$\Delta_g = (f-2)(f+1)^{g-1} + 1. \tag{10}$$

3.2. Spectrum of pRHF

We determine the eigenvalue spectrum of $\mathbf{A_p}$ for pRHF by extending the decimation method [12], developed for $\gamma = 0$, to the case $\gamma \neq 0$. As discussed in section 3.1, the procedure to obtain the eigenvalues of generation g consists of $g-1$ iterative steps. For pRHF the situation is different in the last iteration. In this iteration, we transform $(f+1)^{g-1}$ regular beads to $(f+1)^{g-1}$ jointed star structures whose fCC are perturbed. Thus, whilst equation (4) holds for the first $g-2$ iterations, for the last one we must find another equation which takes into account this difference in the procedure used to determine the spectrum of the matrix $\mathbf{A_p}$. The proof is provided for arbitrary f, although in figures 2, 3 and 4 we represent the special case $f = 4$. The proof uses the fact that there are three kinds of beads: fCC, beads on connecting bonds and beads at the end of dangling bonds. For a particular fCC (which is a trap), we have

$$(f + \mathrm{i}\gamma - \lambda)\phi_0 - \sum_{j=1}^{f} \phi_j = 0, \tag{11}$$

where ϕ_0 is the eigenvector component referred to the center bead and ϕ_j are the eigenvector components of its nearest neighbors. These nearest neighbors (if not peripheral) appear doubly coordinated:

$$(2-\lambda)\phi_j - \phi_0 - \phi_m = 0, \tag{12}$$

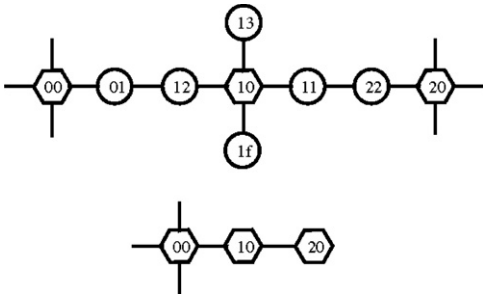

Figure 3. Decimation step for doubly coordinated centers, following figure 15 of [12].

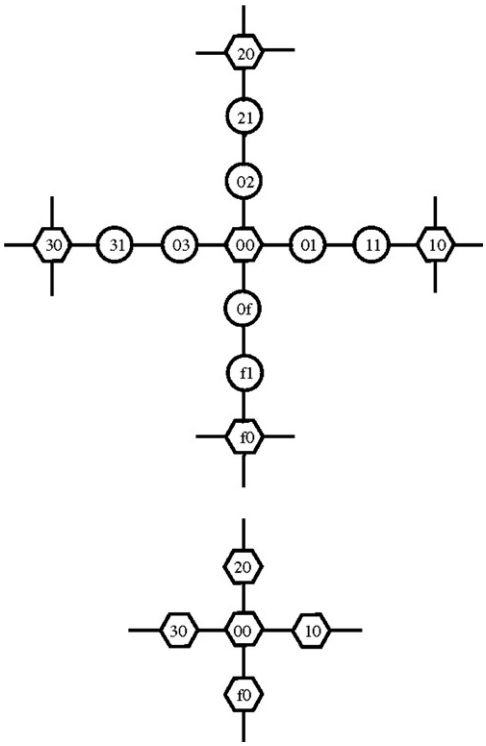

Figure 4. Decimation step for f-coordinated centers, following figure 16 of [12].

where ϕ_0 is the eigenvector component of the fCC neighbor of j and ϕ_m denotes the component of the two-coordinated neighbor of j. The last case is referred to a peripheral bead component ϕ_j:

$$(1-\lambda)\phi_j - \phi_0 = 0. \tag{13}$$

Via the decimation procedure [12] the nodes represented by an open circle will disappear in order to obtain the lowest set of the figure. Figure 2 represents the decimation step for singly coordinated centers. For this situation the eigenvalue equations read

$$(1-\lambda)\phi_{1j} = \phi_{10} \qquad \text{for} \quad 2 \leqslant j \leqslant f, \tag{14}$$

$$(f + i\gamma - \lambda)\phi_{10} = \phi_{11} + \sum_{j=2}^{f} \phi_{1j}, \tag{15}$$

$$(2 - \lambda)\phi_{11} = \phi_{01} + \phi_{10} \tag{16}$$

and

$$(2 - \lambda)\phi_{01} = \phi_{00} + \phi_{11}. \tag{17}$$

The solution of this system of linear equations is given by

$$\phi_{00} = \{[(2-\lambda)^2 - 1][(f-\lambda) - (f-1)(1-\lambda)^{-1}] - (2-\lambda) + i\gamma[(2-\lambda)^2 - 1]\}\phi_{10}. \tag{18}$$

Thus, equation (18) in terms of $P(\lambda)$ is

$$\phi_{00} = [1 - P(\lambda) + i\gamma(\lambda^2 - 4\lambda + 3)]\phi_{10} = [1 - P^*(\lambda)]\phi_{10}, \tag{19}$$

where $P^*(\lambda) = P(\lambda) - i\gamma(\lambda^2 - 4\lambda + 3)$ and $P(\lambda)$ is given by equation (3). We consider now the case of two-coordinated beads, as illustrated in figure 3. Here, the components of the beads that remain after decimation are ϕ_{00}, ϕ_{10} and ϕ_{20}, and others (represented by open circles) will disappear. The eigenvalue equations are

$$(2 - \lambda)\phi_{01} = \phi_{00} + \phi_{12}, \tag{20}$$

$$(2 - \lambda)\phi_{12} = \phi_{01} + \phi_{10}, \tag{21}$$

$$(1 - \lambda)\phi_{1j} = \phi_{10} \qquad \text{for} \quad 3 \leqslant j \leqslant f, \tag{22}$$

$$(f + i\gamma - \lambda)\phi_{10} = \phi_{11} + \phi_{12} + (f-2)\phi_{13}, \tag{23}$$

$$(2 - \lambda)\phi_{11} = \phi_{22} + \phi_{10} \tag{24}$$

and

$$(2 - \lambda)\phi_{22} = \phi_{11} + \phi_{20}. \tag{25}$$

By playing around with these equations, we obtain the solution

$$\phi_{00} + \phi_{20} = [2 - P^*(\lambda)]\phi_{10}. \tag{26}$$

The case of fCC is shown in figure 4. After the decimation procedure only the fCC will survive. The eigenvalue problem is given by the equations

$$(2 - \lambda)\phi_{j1} = \phi_{0j} + \phi_{j0} \qquad \text{for} \quad 1 \leqslant j \leqslant f \tag{27}$$

$$(2 - \lambda)\phi_{0j} = \phi_{00} + \phi_{j1} \qquad \text{for} \quad 1 \leqslant j \leqslant f \tag{28}$$

and

$$(f - \lambda)\phi_{00} = \sum_{j=1}^{f} \phi_{0j}. \tag{29}$$

The solution of this system of equations is

$$\sum_{j=1}^{f} \phi_{0j} = [f - P^*(\lambda)]\phi_{00}. \tag{30}$$

Thus, as in the case of the uperturbed regular hyperbranched fractal, the eigenvalues of generation $g + 1$ are given by the eigenvalues of generation g, solving the equation

$$P^*\left(\lambda_i^{(g+1)}\right) = \lambda_i^{(g)}. \tag{31}$$

Thus, the whole eigenvalue spectrum can be determined analytically, by knowing the eigenvalues of the small unperturbed RHF of generation $g = 1$.

For the pRHF the eigenvalues of generation g, denoted by λ_g, will be determined by the eigenvalues of generation $g-1$, $\lambda_{g-1} = a$ of the unperturbed RHF, simply by solving the third-order polynomial:

$$\lambda_g^3 - (f + 4 + \mathrm{i}\gamma)\lambda_g^2 + [3(f+1) + 4\mathrm{i}\gamma]\lambda_g - 3\mathrm{i}\gamma - a = 0. \tag{32}$$

It is simple to see that equation (32) is reduced to equation (4), corresponding to the unperturbed RHF, by taking $\gamma \to 0$. For the cases in which $\gamma \neq 0$, we checked numerically the correctness of this equation by comparing until generation $g = 5$ the analytical results (implemented in a program written in the OCTAVE language [26]) with the numerical diagonalization of $\mathbf{A_p}$ provided by the Fortran routine CS [27]. Besides the values obtained through equation (32), we have two further non-degenerate eigenvalues given by the solution of $\lambda^2 - (f + 1 + \mathrm{i}\gamma)\lambda + \mathrm{i}\gamma = 0$, which replace the values 0 and $f+1$ of the unperturbed RHF. The degeneracy of the eigenvalues will depend on the generation when they appeared for the first time. Knowing the exact analytical spectrum of the pRHF we will turn our attention to use it for some applications.

4. Results

The dynamics of the general Gaussian structures can be described by a set of linearized Langevin equations for all the position vectors $\mathbf{R}_n$ of the nth bead of the structure:

$$\zeta \frac{\mathrm{d}\mathbf{R}_n(t)}{\mathrm{d}t} + K \sum_{m=1}^{N} A_{nm}\mathbf{R}_m(t) = \mathbf{f}_n(t) + \mathbf{F}_n(t), \tag{33}$$

where ζ is the friction constant of the beads, K is their elasticity constant and $\mathbf{A}$ is the connectivity matrix. The stochastic forces $\mathbf{f}_n(t)$ are assumed to be Gaussian, with $\langle \mathbf{f}_n \rangle = 0$ and $\langle \mathbf{f}_{n\alpha}(t)\mathbf{f}_{m\beta(t')}\rangle = 2k_BT\zeta\delta_{nm}\delta_{\alpha\beta}\delta(t-t')$ (α and β denote the x, y and z directions).

We focus on the motion of the general Gaussian structures under a constant external force $\mathbf{F} = F\theta(t-0)\mathbf{e}_y$, switched on at $t = 0$ and acting on a single bead in the y direction. The displacement averaged over the fluctuating forces $\mathbf{f}_n(t)$ and over all the beads of the structure is given by [3, 11, 23]

$$\overline{Y}(t) = \frac{F}{\zeta N}t + \frac{F\tau_0}{\zeta N}\sum_{j=2}^{N}\frac{1 - \exp(-\lambda_j t/\tau_0)}{\lambda_j}. \tag{34}$$

As seen in section 3.2, for a perturbed RHF, because of the non-hermiticity of the operator $\mathbf{A_p}$ which replaced $\mathbf{A}$, the eigenvalues can be written as $\lambda_j = \epsilon_j + \mathrm{i}\delta_j$. Thus the average displacement, given by equation (34), is a complex number and can be split in a real component and an imaginary one:

$$\overline{Y}(t) = \Re(\overline{Y}(t)) + \mathrm{i}\Im(\overline{Y}(t)), \tag{35}$$

where

$$\Re(\overline{Y}(t)) = \frac{F}{\zeta N}t + \frac{F\tau_0}{\zeta N}\sum_{j=2}^{N}\frac{\epsilon_j - \exp(-\epsilon_j t/\tau_0)[\epsilon_j\cos(\delta_j t/\tau_0) - \delta_j\sin(\delta_j t/\tau_0)]}{\epsilon_j^2 - \delta_j^2} \tag{36}$$

$$\Im(\overline{Y}(t)) = \frac{F\tau_0}{\zeta N}\sum_{j=2}^{N}\frac{-\delta_j + \exp(-\epsilon_j t/\tau_0)[\delta_j\cos(\delta_j t/\tau_0) + \epsilon_j\sin(\delta_j t/\tau_0)]}{\epsilon_j^2 - \delta_j^2}. \tag{37}$$

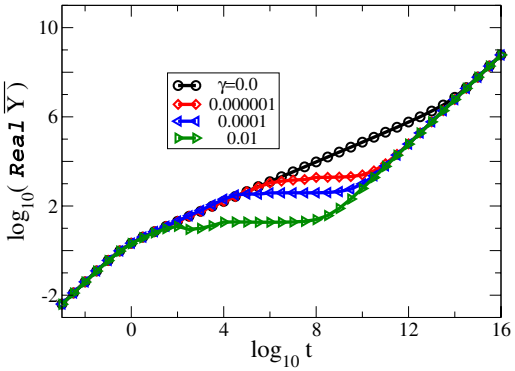

Figure 5. The real part of the averaged displacement, equation (36), for pRHF of functionality $f = 3$ and generation $g = 13$ with the strength of the trap being $\gamma = 0$, 10^{-6}, 10^{-4} and 0.01.

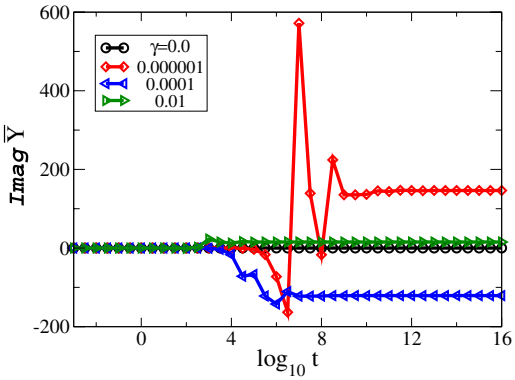

Figure 6. The imaginary part of the averaged displacement, equation (37), for pRHF of functionality $f = 3$ and generation $g = 13$ with the strength of the trap being $\gamma = 0$, 10^{-6}, 10^{-4} and 0.01. The continuous lines are kept only to give a feeling of the curves.

It can be easily seen that if $\gamma = 0$, implying that all $\delta_j \to 0$, the imaginary part of the displacement vanishes while the real part will have the known form of the unperturbed RHF [12].

In figure 5 we plot in the double logarithmical scale the real part of the average displacement for pRHF of functionality $f = 3$ and generation $g = 13$. The constants were set to $F/\zeta = 1$ and $\tau_0 = 1$. In the region of very short times $\overline{Y}(t) = Ft/\zeta$, which corresponds to the situation when only one monomer moves, and in the limit of very long times $\overline{Y}(t) = Ft/N\zeta$, when the whole structure drifts. In the intermediate time domain the topology of the structure will come into play. For $\gamma = 0$ a scaling region is easily seen, as spotted before by one of the authors [12]. When γ increases, this scaling region will disappear, even for small values of the trap strength $\gamma = 10^{-6}$ or 10^{-4}.

Figure 6 shows, in the semi-logarithmical scale, the imaginary part of the average displacement for pRHF of functionality $f = 3$ and generation $g = 13$. If $\gamma = 0$ the imaginary part of the average displacement, $\Im(\overline{Y}(t))$, is equal to 0, as expected. Although the physical meaning of this quantity for $\gamma \neq 0$ is difficult to assess, some qualitative remarks can

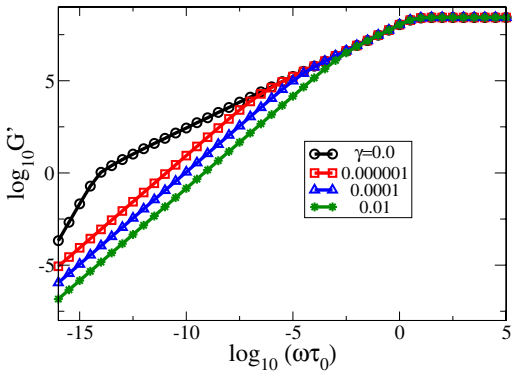

Figure 7. Storage modulus G' for RHF of functionality $f = 3$ and generation $g = 14$ where the strength of the trap is $\gamma = 0, 10^{-6}, 10^{-4}$ and 0.01.

be drawn. One can observe that for very long times $\Im(\overline{Y}(t))$ is a constant dependent on the imaginary and the real part of the whole eigenvalue spectrum:

$$\Im(\overline{Y}(t)) \to -\frac{F\tau_0}{\zeta N}\sum_j \frac{\delta_j}{\epsilon_j^2 - \delta_j^2}. \tag{38}$$

It was observed that the imaginary components of *all* the complex eigenvalues, δ_j, will increase by increasing γ (this happens in the range of small γ values, see [29] for details of this specific case and [21, 22] for similar situations), making possible that the sum from equation (38) changes its sign. In figure 6, in the limit of very long times, this change is clearly noticed.

Another quantity which may be accessed through micromechanical manipulations [24] is the mechanical and dielectric relaxation. In the mechanical experiments the complex dynamic modulus $G^*(\omega)$, i.e. its real (the storage) $G'(\omega)$ and imaginary (the loss) $G''(\omega)$ components [12, 16], is analyzed. Disregarding the constants present in its mathematical expression, G^* appears as

$$G^*(\omega) = G'(\omega) + \mathrm{i}G''(\omega) = \sum_j \frac{\omega^2/\lambda_j^2 + \mathrm{i}\omega/\lambda_j}{1 + \omega^2/\lambda_j^2}. \tag{39}$$

Again, we write the eigenvalues as $\lambda_j = \epsilon_j + \mathrm{i}\delta_j$ and after some calculations we obtain the storage and the loss modulus for complex eigenvalues:

$$G'(\omega) = \sum_j \frac{\omega^4 - \omega^3\delta_j + \omega^2(\epsilon_j^2 - \delta_j^2) + \omega\delta_j(\epsilon_j^2 + \delta_j^2)}{(\omega^2 + \epsilon_j^2 + \delta_j^2)^2 - 4\omega^2\delta_j^2} \tag{40}$$

and

$$G''(\omega) = \sum_j \frac{\omega^3\epsilon_j - 2\omega^2\epsilon_j\delta_j + \omega\epsilon_j(\epsilon_j^2 + \delta_j^2)}{(\omega^2 + \epsilon_j^2 + \delta_j^2)^2 - 4\omega^2\delta_j^2}. \tag{41}$$

In equations (40) and (41), if we take $\gamma \to 0$, thus all $\delta_j \to 0$, we obtain the well-known expressions [11, 12]. In figures 7 and 8, we plot in double logarithmic scales to base 10 the storage and the loss modulus for RHF of functionality $f = 3$ and generation $g = 14$. In the very low frequency limit the storage modulus $G'(\omega)$ shows an ω^2 dependence, whereas the loss modulus $G''(\omega)$ increases linearly with ω. In the limit of high frequencies

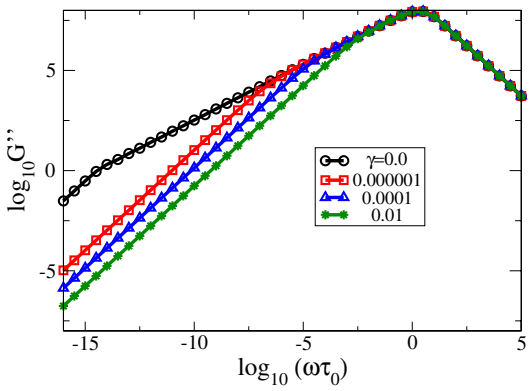

Figure 8. Loss modulus G'' for RHF of functionality $f = 3$ and generation $g = 14$ where the strength of the trap is $\gamma = 0, 10^{-6}, 10^{-4}$ and 0.01.

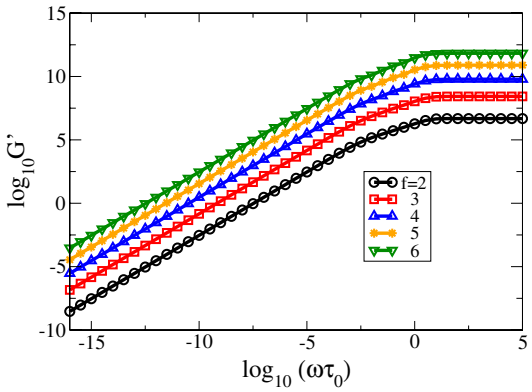

Figure 9. Storage modulus G' for RHF of functionality $f = 2, 3, 4, 5$, and 6, and of generation $g = 14$ where the strength of the trap is $\gamma = 0.01$ for all the curves.

$G'(\omega)$ shows a plateau behavior, whereas $G''(\omega)$ decays, after showing a maximum, with ω^{-1}. In the intermediate region the topology of the structure and the influence of the traps will come into play. For the case of no trap in the structure, we observe a scaling region in this intermediate region. This slope is given by $\tilde{d}/2 = \ln(f + 1)/\ln(3f + 3)$ which manifests the scaling of the fractal, see [16]. By inserting in the fCC the traps we can easily note that even for a very small trap's strength (10^{-6}) the behavior is drastically different. The scaling region becomes smaller when γ increases, and for $\gamma > 0.01$ it will completely disappear.

In figure 9 we display the storage modulus, equation (40), for RHFs of generation $g = 14$ and functionalities $f = 2, 3, 4, 5$ and 6, corresponding to structures ranging from $N = 2^{14}$ to $N = 6^{14}$. For all the cases we have the same strength of the traps: $\gamma = 0.01$. We stop to note that in the intermediate frequency regime a well-defined scaling region was observed for $\gamma = 0$, for all the values of f. In the case depicted in figure 9, even for a small perturbation strength, such as $\gamma = 0.01$, this scaling region has been drastically shortened, for all the functionalities studied.

5. Conclusions

In this work we focused on the eigenvalue spectrum of the perturbed regular hyperbranched fractals, i.e. RHF with traps in the fCC, as depicted in figure 1. The perturbation has been taken into account by introducing a complex contribution to the influenced beads. Although we had to deal with complex numbers, we have been able to determine analytically the full spectrum of the operator $\mathbf{A_p}$. We used this spectrum to calculate some useful quantities, such as storage and loss moduli, and the average displacement.

For the storage and the loss moduli, we observed that even a small perturbation strength, such as $\gamma = 10^{-6}$, will have a big influence. The scaling in the intermediate region, observed for unperturbed RHF, will start to shorten while increasing γ, and for $\gamma > 0.01$ it will completely disappear. For pRHF the average displacement can be split into two components, the real and the imaginary part. For the real component the behavior for the extremal (very short and very long) time regimes was as expected, namely a linear dependence. In the intermediate time domain the traps destroyed the scaling observed for unperturbed RHF. We are confident that such macroscopic observables, such as mechanical relaxation and the average displacement even in very small perturbative terms (i.e. non-comparable in magnitude with the matrix elements of $\mathbf{A}$), may reveal much about the underlying microscopic structures.

Acknowledgments

The authors would like to thank Professor Dr Alexander Blumen for fruitful discussions. AV gratefully acknowledges Professor Federico Magnani for a grant of the CIRCE project. MG acknowledges a grant of CNPq. AJ acknowledges the grant PN II RP-14 Nr.2/01.07.2009. AJ would like to thank the group 'Simulation laboratory of nanostructured systems' from the Faculty of Physics, Babes-Bolyai University, for using the lab facilities.

References

[1] Rouse P E 1953 *J. Chem. Phys.* **21** 1272
[2] Zimm B H 1956 *J. Chem. Phys.* **24** 269
[3] Biswas P, Kant R and Blumen A 2000 *Macromol. Theory Simul.* **9** 56
[4] Kant R, Biswas P and Blumen A 2000 *Macromol. Theory Simul.* **9** 608
[5] Gurtovenko A A, Gotlieb Yu Ya and Blumen A 2002 *Macromolecules* **35** 7481
[6] Cai C and Chen Z Y 1997 *Macromolecules* **30** 5104
[7] Gurtovenko A A, Markelov D A, Gotlib Yu Ya and Blumen A 2003 *J. Chem. Phys.* **119** 7579
[8] Ganazzoli F, La Ferla R and Raffaini G 2001 *Macromolecules* **34** 4222
[9] Jayanthi C S, Wu S Y and Cocks J 1992 *Phys. Rev. Lett.* **69** 1955
[10] Jayanthi C S and Wu S Y 1993 *Phys. Rev.* B **48** 10188
Jayanthi C S and Wu S Y 1993 *Phys. Rev.* B **48** 10199
Jayanthi C S and Wu S Y 1994 *Phys. Rev.* B **50** 897
[11] Blumen A, Jurjiu A, Koslowski Th and von Ferber Ch 2003 *Phys. Rev.* E **67** 061103
[12] Blumen A, von Ferber Ch, Jurjiu A and Koslowski Th 2004 *Macromolecules* **37** 638
[13] Gurtovenko A A and Blumen A 2005 *Adv. Polym. Sci.* **182** 171
[14] Sommer J-U and Blumen A 1995 *J. Phys. A: Math. Gen.* **28** 6669
[15] Bunde A and Havlin S (eds) 1996 *Fractals and Disordered Systems* (Berlin: Springer)
[16] Doi M and Edwards S R 1986 *The Theory of Polymer Dynamics* (Oxford: Clarendon)
[17] Aharonov Y, Davidovich L and Zagury N 1993 *Phys. Rev.* A **48** 1687
[18] Fahri E and Gutmann S 1998 *Phys. Rev.* A **58** 915
[19] Kempe J 2003 *Contemp. Phys.* **44** 307
[20] Sakurai J 1993 *Modern Quantum Mechanics* 2nd edn (Redwood City, CA: Addison-Wesley)
[21] Mülken O, Blumen A, Amthor T, Giese C, Reetz-Lamour M and Weidemüller M 2007 *Phys. Rev. Lett.* **99** 090601

[22] Volta A 2009 *J. Phys. A: Math. Theor.* **42** 225003
[23] Biswas P, Kant R and Blumen A 2001 *J. Chem. Phys.* **114** 2430
[24] Granek R and Klafter J 2001 *Europhys. Lett.* **56** 15
[25] Cullum J K and Willoughby R 1985 *Lanczos Algorithms for Large Symmetric Eigenvalue Problems, vol I: Theory, vol II: Programs* (Boston: Birkäuser)
[26] Eaton J W *GNU Octave Manual* www.octave.org
[27] Bar-On I and Ryaboy V 1997 *SIAM J. Sci. Comput.* **18** 1412
[28] Bronstein I N and Semendjajev K A 1985 *Taschenbuch der Mathematik (Handbook of Mathematics)* (Moscow and Leipzig, Germany: Nauka and Teubner) chapter 2.4.2
[29] Volta A 2009 Classical and quantum dynamics on hyperbranched networks *Doctoral dissertation* Albert-Ludwigs-Universität, Freiburg im Breisgau (http://www.freidok.uni-freiburg.de/volltexte/7104/)